

${}^4\text{He}(\gamma, p)\text{-to-}(\gamma, n)$ cross-section ratio

T. W. Phillips, B. L. Berman, and D. D. Faul

Lawrence Livermore Laboratory, University of California, Livermore, California 94550

J. R. Calarco and J. R. Hall

Stanford University, Stanford, California 94305

(Received 14 August 1978)

We have measured the cross-section ratio $\sigma(\gamma, {}^3\text{H})/\sigma(\gamma, {}^3\text{He})$ for ${}^4\text{He}$ from 31 to 51-MeV with an incident bremsstrahlung beam and a collimated solid-state telescope at 90° laboratory angle. The results obtained from these data for the total cross-section ratio are consistent with unity for most of the energy range covered, but deviate from this value in the energy region near 44 MeV.

NUCLEAR REACTIONS ${}^4\text{He}(\gamma, {}^3\text{H}, {}^3\text{He})$, $E_\gamma=31-51$ MeV; measured differential cross-section ratio at 90° (laboratory); deduced total $(\gamma, p)\text{-to-}(\gamma, n)$ cross-section ratio.

I. INTRODUCTION

The ratio of the photoproton and photoneutron cross sections for ${}^4\text{He}$ has been a subject of considerable controversy during the last several years. This ratio is important because it is a sensitive indicator of the degree of isospin mixing which is present in the simple ${}^4\text{He}$ nucleus, and thus provides one with a quantitative test of the degree to which the charge symmetry of the nuclear force might be broken. The controversy concerns the wide disparity in values reported for this ratio and for the (γ, n) cross section in particular. [There is general agreement for the (γ, p) cross section in the energy range of greatest interest.]

The controversy was initiated by Berman, Fultz, and Kelly (BFK),^{1,2} who reported their measurement of ${}^4\text{He}(\gamma, n)$ from threshold to 31 MeV with monoenergetic photons and a liquid helium sample at Livermore. The values BFK obtained for $\sigma(\gamma, n)$, which peaked at about 1 mb for photon energies E_γ from about 25 to 27 MeV, were not much more than half those for $\sigma(\gamma, p)$. This led them to point out the possible implication mentioned above, namely, that unless there were an unexpectedly large amount of Coulomb mixing throughout the giant-resonance region, there would have to be a small but nonzero violation of charge symmetry. Prior to the experiment of BFK, there were four ${}^4\text{He}(\gamma, n)$ measurements reported, all done with bremsstrahlung and all having large uncertainties—Ferguson *et al.*,³ whose $\sigma(\gamma, n)$ values were slightly higher than those of BFK, but covered the energy range only up to 25 MeV, Gorbunov,⁴ whose values were much higher than those of BFK at all energies

and were comparable to the (γ, p) values, and Ferrero *et al.*⁵ and Busso *et al.*,^{6,7} whose $\sigma(\gamma, n)$ values were in essential agreement with those of BFK up to about 27 MeV, but then rose sharply to meet those of Gorbunov at about 29 MeV. One ${}^3\text{He}(n, \gamma)$ cross-section value, at ~ 24 MeV, also had been published⁸; it agreed with the work of BFK.

Several other experiments were undertaken to check the BFK results. Berman, Firk, and Wu (BFW)⁹ measured $d\sigma(\gamma, n)/d\Omega|_{90^\circ}$ up to 32 MeV with bremsstrahlung photons and a liquid sample at Yale and found essentially the same (low) ${}^4\text{He}(\gamma, n)$ cross section as BFK. Irish *et al.*^{10,11} measured the differential (γ, n_0) cross section at six angles up to 32 MeV with bremsstrahlung and a liquid sample at Toronto; in doing so, they essentially duplicated the measurement of BFW, and reproduced the results of BFK and BFW. Meanwhile, however, two measurements were reported which cast serious doubt on the Livermore, Yale, and Toronto results. At Saskatchewan, Shin and his collaborators^{12,13} measured the differential (γ, n) cross section at five angles up to 70 MeV with bremsstrahlung and a liquid sample and obtained results in agreement with Gorbunov [and the (γ, p) values]; and at the National Bureau of Standards, Dodge and Murphy¹⁴ determined the $(\gamma, p)\text{-to-}(\gamma, n)$ differential cross-section ratio at 90° in the laboratory from 30 to 50 MeV from sequential measurements of the ${}^3\text{H}$ and ${}^3\text{He}$ particles from the electrodisintegration of ${}^4\text{He}$ by a 90-MeV electron beam with a gaseous helium sample, and obtained results consistent with unity in this energy range. These results prompted Irish *et al.*^{15,16} to remeasure the 98° differential (γ, n_0) cross section with a gaseous

sample, obtaining results in substantial agreement with the (γ, p) values, and later to demonstrate¹⁷ that the earlier Yale and Toronto (but not Livermore) results very likely could be explained by a dependence of the density of the liquid samples on the bremsstrahlung beam intensity.

The situation at this time was summarized by Hanna,¹⁸ who concluded that the "consensus" values for the (γ, n_0) cross section were in agreement with those for the (γ, p_0) cross section, but cautioned that he did "not consider the matter to be entirely settled". At this point, we determined that another attempt should be made to measure the (γ, p) -to- (γ, n) cross-section ratio for an energy range spanning the region from 27 to 50 MeV (if possible), with *real* photons and a *gaseous* sample, and with *simultaneous* measurement of the ^3H and ^3He product particles with the same detector. We therefore undertook such a measurement which seemed to us to encompass the best features of several previous measurements and to add to them the simultaneity requirement, in an effort to throw additional light on this problem. We succeeded in performing this experiment, but only down to 31 MeV in energy, so that the overlap with many of the earlier measurements was not all that we desired. We report on this experiment here.

II. EXPERIMENT AND DATA REDUCTION

The experiment was performed at the Lawrence Livermore Laboratory Electron-Positron Linear Accelerator facility, using the bremsstrahlung beam which was produced when a beam of 56-MeV electrons from the accelerator was allowed to strike a 0.05-mm-thick platinum target. The experimental setup is shown in Fig. 1. The electrons which passed through the target were swept into a 5-m-deep dump hole in the floor by a bending magnet. The forward bremsstrahlung beam was collimated by a 10-cm-thick, 1.27-cm-diameter lead collimator embedded in a 10-cm-

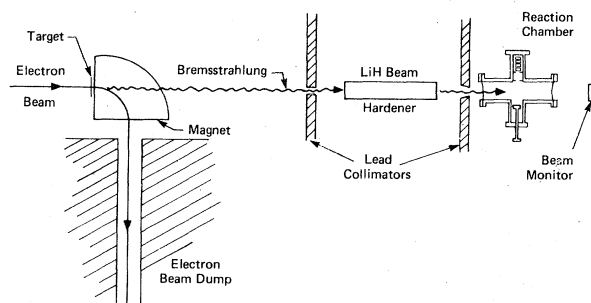


FIG. 1. Schematic diagram of the experimental layout.

thick lead shielding wall, passed through a 60-cm-thick low- Z beam hardener to reduce the flux of (unwanted) low-energy photons, and collimated again by a 10-cm-thick tapered lead collimator (its upstream diameter was 1.59 cm and its downstream diameter was 1.27 cm) just before entering the helium-filled reaction chamber. The photon beam was monitored downstream from the reaction chamber with a small NaI(Tl) detector. (It should be noted here that since this was a counting-rate ratio experiment, measurement of the absolute photon flux was not required.)

Details of the reaction chamber are shown in Fig. 2. The entrance and exit windows were made of aluminized Mylar, 5 cm in diameter and 0.025 mm thick. The counter telescope (see below) was located in an arm of the chamber at 90° to the incident photon beam direction, and was protected from external sources of background by local lead shielding. Tantalum collimators of various diameters were located between the counter telescope and the volume of helium gas irradiated by the collimated photon beam (see Fig. 2). Opposite to the counter telescope, a radioactive ^{241}Am alpha-particle source, used for calibration purposes, was mounted on a plunger in another arm of the reaction chamber, so that the ^{241}Am source could be retracted when not in use.

The use of a bremsstrahlung spectrum produced no problem in the determination of the energy of the photon which induced the reaction. Instead of protons and neutrons, ^3He and ^3H nuclei were detected and identified in the multi-counter telescope. This ensured the observation of only the two-body breakup cross section, and thus the photon energy was determined from the energy of the outgoing trinucleon by kinematics.

The telescope consisted of four silicon diodes in the order $5\ \mu\text{m}$, $17\ \mu\text{m}$, $500\ \mu\text{m}$, and $500\ \mu\text{m}$. ^3He particles of less than about 8 MeV were stopped in the $17\text{-}\mu\text{m}$ detector and identified by comparing the outputs of the $5\text{-}\mu\text{m}$ and $17\text{-}\mu\text{m}$ detectors. Tritons, on the other hand, of energy greater than about 2 MeV, lost negligible energy in the $5\text{-}\mu\text{m}$ detector but were detected and identified using the $17\text{-}\mu\text{m}$ first $500\text{-}\mu\text{m}$ detectors. The last $500\text{-}\mu\text{m}$ detector was used in anticoincidence with the first three in order to eliminate electrons (which made up the bulk of the background in this experiment), which were produced by pair production in the target as well as in the chamber walls and elsewhere.

The target was ^4He gas maintained at a pressure of either 0.10 or 0.25 atm. The telescope was operated inside the gas to eliminate any energy loss of the trinucleons in foil windows. After taking into account all energy losses in the gas

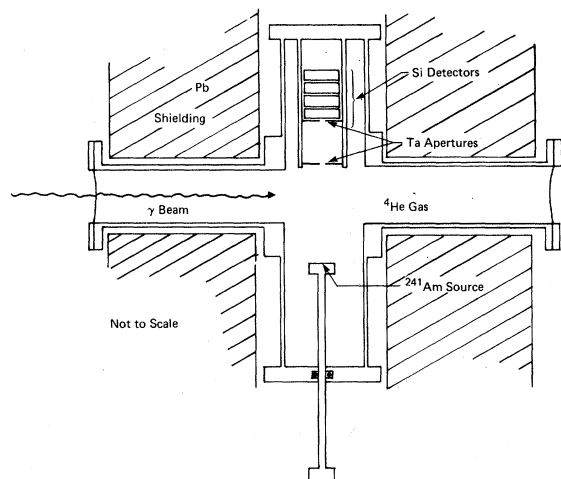


FIG. 2. Schematic diagram of the reaction chamber and the collimated counter-telescope detector system.

as well as in the 5- μm detector, the lower-energy limit for observing ${}^3\text{He}$ particles was about 2 MeV.

A simplified block diagram of the electronic circuitry used is shown in Fig. 3. A coincidence between a signal from the 17- μm detector and either the 5- μm detector or the first 500- μm detector generated a gate (unless a veto signal was present from the last 500- μm detector) which allowed the linear signals from the first three detectors to pass on to three analog-to-digital converters. The digitized signals from the three analog-to-digital converters were stored as 36-bit words on a three-million word magnetic drum by an on-line data-acquisition system. On-line sorting of the detected events into a two-

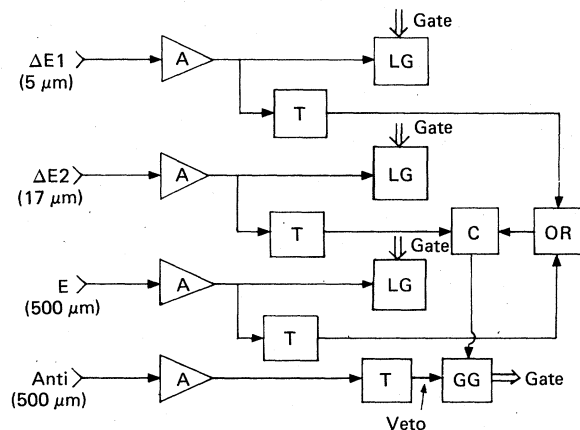


FIG. 3. Simplified block diagram of the counter-telescope detector electronics. The four silicon detectors are labeled $\Delta E1$, $\Delta E2$, E , and Anti ; A —amplifiers; T —triggers; LG —linear gates; C —coincidence circuit; GG —gate generator; OR —or circuit.

dimensional array and subsequent display of the sorted data provided information on the progress of the experiment.

The main problem to overcome was the detection of charged particles during the intense beam burst from the Linac, when there were many background electrons and photons present. In order overcome this high background rate, the accelerator was operated at its maximum duty factor of 0.2% (720 pulses/sec of 3- μs width) and the output signals from the preamplifiers from each detector in the counter telescope were clipped just when they peaked. This preserved the amplitude information but clamped the outputs to zero as soon as possible. The clipped outputs were amplified to ORTEC timing-filter amplifiers with integration time constants of about 20 ns, and then passed through ORTEC 442 peak-stretching gates opened by the coincidence. This method allowed the system to operate at high rates without significant pileup or pulse-pair resolution problems. However, clipping and amplifying with net time constants as short as 50 to 100 ns increased the noise level relative to the signal height and degraded the resolution significantly, particularly for the 5- μm detector, where the noise level already was high owing to its large capacitance. Resolution from the 5- μm detector was only about 300 keV, producing a 5-to-10% uncertainty from 5.5-MeV α particles from ${}^{241}\text{Am}$.

The linearity of the electronic circuitry was checked by injecting pulser pulses into the preamplifiers of the telescope and using calibrated attenuators to cover the range of the experiment. The energy calibration was obtained by evacuating the target chamber and observing α -particle events from the ${}^{241}\text{Am}$ source.

It was found in tests of the counter telescope using the ${}^3\text{He}(p, p)$ and (p, n) reactions at the Stanford University Tandem Van de Graaff accelerator that tight collimation was required to prevent multiple scattering in the counter telescope from distorting the ratio measurements. This was achieved by positioning two tantalum apertures in front of the counter telescope as shown in Fig. 2, the one nearer the telescope having a diameter of 2.38 mm and the one nearer the interaction volume having a diameter of 4.76 mm. The consequent low counting rate made separation of the ${}^3\text{He}$ events from ${}^1\text{H}$ and noise events impossible at energies below $E_\gamma = 39$ MeV. In order to obtain results at lower energies, the ${}^3\text{H}$ data from a run with more open collimation were normalized above 39 MeV to the ${}^3\text{H}$ data obtained with tight collimation. The normalized ${}^3\text{H}$ data and the ${}^3\text{He}$ data obtained with tight col-

limation were used to extend the useful energy range down to 31 MeV.

Three-dimensional projections of part of the data are shown in Figs. 4 and 5. Plots such as Fig. 4, in which the energy deposited in the two (thin) front detectors is plotted against the total energy deposited, were used to obtain the ^3H yield (note the clean separation of ^3H events from ^1H events); plots such as Fig. 5, in which the energy deposited in the front (thinnest) detector is plotted against the total energy deposited, were used to obtain the ^3He yield (in this kind of plot the ^3H and ^1H events overlap with each other and with low-amplitude noise signals). From these data, with proper account taken of the pressure, the energy loss of the ^3H and ^3He particles in the gas and in the detectors, and the size of the interaction volume and solid angles involved, the differential cross-section ratio was determined.

The factor which placed a low-energy limit on the cross-section ratio was not the energy loss

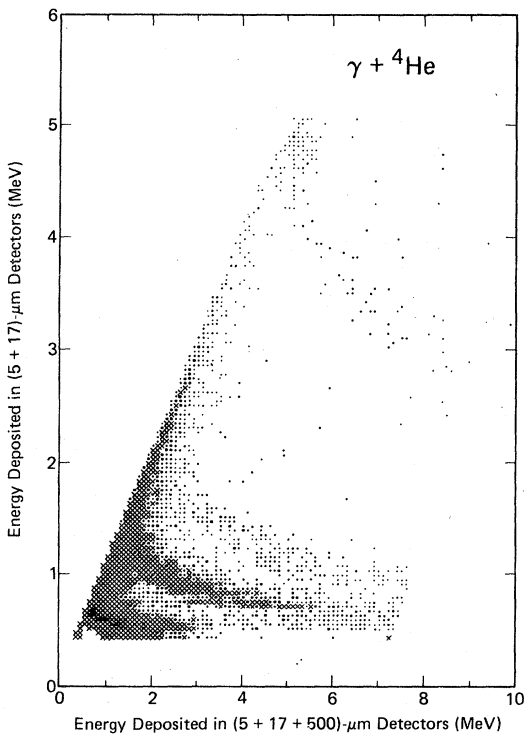


FIG. 4. Three-dimensional representation of the $\gamma + ^4\text{He}$ data obtained from the 3-detector telescope (5, 17, and 500 μm thick). The third dimension (number of events) is represented by the darkness of the character plotted for each bin. From the top of the plot the four trajectories corresponding to ^3He , ^3H , ^4H , and noise events are visible, extending down and to the right. These data were obtained with open collimation at a ^4He gas pressure of 0.10 atm.

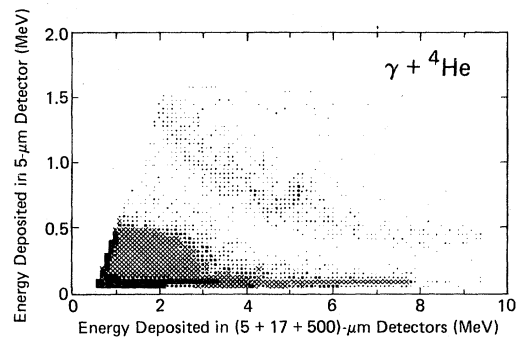


FIG. 5. Three-dimensional representation of the $\gamma + ^4\text{He}$ data, plotting the response of the 5- μm detector only against the total energy loss in the telescope. The third dimension is represented as in Fig. 4. The trajectory of ^3He events only is visible in this projection. These data were obtained with tight collimation at a gas pressure of 0.25 atm.

of the ^3He ions in the gas or the front detector, as might have been expected, but rather the high background of electron pileup events which prevented the identification of ^3H ions to as low an energy as allowed by the thicknesses of the two ΔE detectors. This "noise" from electron pileup extends upward along the diagonal in Fig. 4 and prevents the ^3H locus from being extended accurately to the diagonal. The diagonal, of course, results from events with no energy loss in the 500- μm E detector. For the case of energetic electrons, these events result from particles scattering out of the 17- μm detector and missing the E detector. The effect of this pileup was to limit the lowest photon energy at which the cross-section ratio could be determined to about 31 MeV.

III. RESULTS AND DISCUSSION

The present results for the (γ, p) -to- (γ, n) differential cross-section ratio, at 90° to the photon beam direction in the laboratory for the detected trinucleons, are shown in Fig. 6, as a function of photon energy. The data span the energy range from 31 to 51 MeV; the most reliable data lie between 39 and 46 MeV, where the data from the two experimental runs described in Sec. II overlap and where the data from both are statistically most significant.

In order to interpret these data in terms of the total (integrated-over-angle) cross sections, it is necessary to transform the results into the center-of-mass frame and then to make use of measured angular-distribution data for both reaction channels to convert them to a total cross-section ratio. For the present measurement (or that of Ref. 14), where the trinucleon was detected

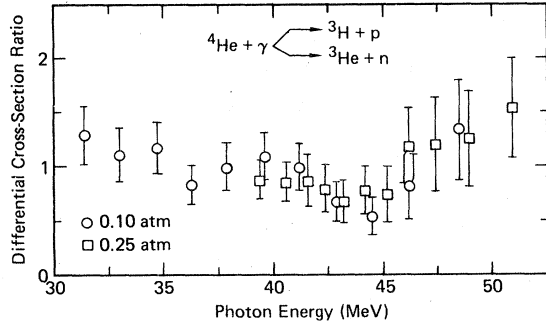


FIG. 6. ${}^4\text{He}(\gamma, p)\text{-to-}(\gamma, n)$ differential cross-section ratio at 90° in the laboratory for the detected trinucleons. The data obtained with a ${}^4\text{He}$ gas pressure at 0.10 atm were normalized to those taken with a pressure of 0.25 atm in the overlap region between 39 and 45 MeV.

at 90° , the corresponding nucleon was emitted at a laboratory angle between 76° and 77° from the photon beam direction; this angle, which reaches a maximum for E_γ equal to twice the threshold energy, or about 40 MeV, is almost independent of energy between 31 and 51 MeV, the energy range of this experiment. This corresponds to center-of-mass angles θ between 79° and 80° for the nucleon (or 100° to 101° for the trinucleon), so that $\cos\theta = 0.186 \pm 0.007$ for all energies of interest here.

It has been the custom among workers in this field to fit differential cross-section data with the expression

$$\frac{d\sigma}{d\Omega} = A + B \sin^2\theta + C \sin^2\theta \cos\theta + D \sin^2\theta \cos^2\theta, \quad (1)$$

so that B gives an indication of the magnitude of the $E1$ strength, D the $E2$ strength, C the interference between the $E1$ and $E2$ components, and A the spin-flip strength. For both the ${}^4\text{He}(\gamma, p)$ and ${}^4\text{He}(\gamma, n)$ cross sections in the energy range of interest here, all measurements have yielded very small (if not vanishing) values for the isotropic term A . These include the (γ, p) measurements of Refs. 4, 19, and 20 and the (γ, n) measurements of Refs. 4, 11, 13, 21, and 22. Like-

wise, the pure quadrupole term D has been shown^{4,13,19} to be very small in this energy range, as is expected from the fact that $E2$ excitation generally is much less probable than $E1$. Therefore, one is well justified (at a level of accuracy of a few percent) in assuming angular distributions in this energy range of the form

$$\frac{d\sigma}{d\Omega} \propto \sin^2\theta(1 + \beta \cos\theta), \quad (2)$$

where $\beta = C/B$.

Table I lists values for the asymmetry coefficient β for photon energies between 31 and 51 MeV for the literature. Data from a few experiments [the (γ, p) data of Ref. 23 and the (γ, n) data of Refs. 4 and 21] are not included in the table because they are sparse or otherwise appear to be of lesser reliability than those included. The adopted values of β for the (γ, p) reaction present no difficulty; for the (γ, n) reaction, however, a more serious problem arises from the virtual-photon ($e, {}^3\text{He}$) measurement of Murphy.²² We have chosen here to adopt values of β for the (γ, n) reaction close to those of the real-photon (γ, n) measurement of the Saskatchewan group,¹² which are supported by the data of Ref. 7, the theoretical prediction of Crone and Werntz,²⁴ and the similar judgment of Meyerhof and Fiarman in their review.²⁵ The authors of Ref. 14 understandably adopted values close to those of Ref. 22; the effect of this choice will be seen below.

Using the adopted values for β given in Table I, values for the asymmetry term in Eq. (2) were computed; representative values for this quantity are given in the fourth column of Table II, along with the resulting differential cross-section ratio (in the fifth column) to be expected if the total (γ, p) and (γ, n) cross sections were equal. The uncertainty in this calculated ratio is not as large as the uncertainty in the values for β because of the fact that $\cos\theta$ is not large. If the values for β were uncertain by ± 0.1 for the (γ, p) reaction and ± 0.2 for the (γ, n) reaction, for example, the uncertainty in this ratio would be about 6%. The measured differential cross-section ratios (Fig.

TABLE I. Values for the asymmetry coefficient β .

Energy (MeV)	For the ${}^4\text{He}(\gamma, p)$ reaction					For the ${}^4\text{He}(\gamma, n)$ reaction					
	Ref. 19	Ref. 7	Ref. 4	Ref. 20	Adopted	Ref. 2	Ref. 11	Ref. 7	Ref. 12	Ref. 22	Adopted
31	0.64		0.58	0.60	0.62	-0.30	-0.25	-0.45	-0.10		-0.25
36		0.80	0.73	0.72	0.73			0	-0.03		-0.02
41			0.82	0.80	0.81			0.20	0.22	-0.36	0.21
46			0.91	0.82	0.88				0.24	-0.24	0.23
51			0.98	0.84	0.93				0.22	-0.12	0.23

TABLE II. Expected differential cross-section ratio.

Energy (MeV)	Reaction	$\cos\theta$	$\beta \cos\theta^a$	$\frac{(1+\beta \cos\theta)_p}{(1+\beta \cos\theta)_n}$
31	(γ, p)	0.186	0.112	1.17
	(γ, n)	0.193	-0.048	
36	(γ, p)	0.180	0.131	1.14
	(γ, n)	0.184	-0.004	
41	(γ, p)	0.179	0.145	1.10
	(γ, n)	0.182	0.038	
46	(γ, p)	0.181	0.159	1.11
	(γ, n)	0.183	0.042	
51	(γ, p)	0.184	0.171	1.12
	(γ, n)	0.186	0.043	

^aComputed with adopted values for β from Table I.

6) then were divided by the value for

$$(1 + \beta \cos\theta)_p / (1 + \beta \cos\theta)_n$$

at each energy, and the resulting total cross-section ratios $\sigma(\gamma, p)/\sigma(\gamma, n)$ are shown in Fig. 7. It can be seen that near the lower-energy limit of our experiment we obtain a result easily consistent with a total cross-section ratio of unity, but at higher energies we do not. Indeed, in the energy region from 42 to about 45 MeV there are six consecutive data points (see Fig. 7) for which the statistical error flags do not overlap unity, thus making it unlikely that $\sigma(\gamma, p)$ is equal to $\sigma(\gamma, n)$ in this energy region. Moreover, contrary to the case which obtains when one has strong isospin mixing²⁶ (as was discussed in detail by BFK^{1,2} and BFW⁹), here $\sigma(\gamma, n)$ exceeds $\sigma(\gamma, p)$ by some 30% or so. On the other hand, for the highest energies measured here (48–51 MeV),

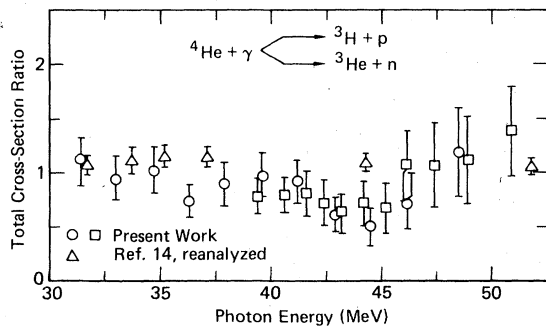


FIG. 7. ${}^4\text{He}(\gamma, p)$ -to- (γ, n) total cross-section ratio. The circles and squares are computed from the measured results shown in Fig. 6 and the angular-distribution parameters given in the tables, under the assumption that Eq. (2) holds. The triangles are data of Ref. 14, reanalyzed under the same conditions; the data points shown at 31.7 and 33.7 MeV represent weighted averages of three and two points, respectively.

it appears that $\sigma(\gamma, p)$ exceeds $\sigma(\gamma, n)$ by 20% or more; but at these high energies the statistical quality of the data is not nearly so good, because of the combined effects of lower cross sections and fewer photons in the bremsstrahlung spectrum near its end point.

Concurrently with the present work, another experiment has been performed, by Balestra *et al.*,²⁷ on the photodisintegration of ${}^4\text{He}$ across the energy region of interest here. This measurement was done with an 85-MeV end-point bremsstrahlung beam, using a diffusion cloud chamber as both sample and detector. Thus, it too was done in such a way as to satisfy the three criteria set out in Sec. I: use of real photons, use of a gaseous sample, and simultaneous detection of both (γ, p) and (γ, n) events with the same detector. The chief disadvantage of this technique is the poor statistical quality of the data, imposed by the low counting-rate capability of the cloud chamber. The results of this measurement, within the statistical uncertainties, agree with those of the present work in the overlapping energy region; for $\sigma(\gamma, p)/\sigma(\gamma, n)$ they obtained $\sim 1.00 \pm 0.08$ for the energy region 31 ± 4 MeV and $\sim 0.95 \pm 0.10$ for 47 ± 12 MeV. Their angular-distribution results are in good agreement with those we adopted (listed in Table I) as well. A more detailed comparison between the two measurements cannot be made, however, since Balestra *et al.* present only the above two data points spanning a 32-MeV energy region. However, they succeeded in obtaining values for the (γ, p) -to- (γ, n) cross-section ratio at lower energies; they present two more data points, $\sim 1.25 \pm 0.08$ at 26 ± 0.5 MeV and $\sim 1.35 \pm 0.10$ at 25 ± 0.5 MeV. These data would seem to establish clearly a rising trend for this ratio with decreasing energy, and lie distinctly higher than the results (of Ref. 4, for example) that are consistent with unity, although still lower than those implied by the work of BFK^{1,2} and BFW.⁹

Lastly, we turn to the results of Dodge and Murphy,¹⁴ who obtained results for $\sigma(\gamma, p)/\sigma(\gamma, n)$ in their virtual-photon measurement consistent with unity throughout this energy range (their average result for ten data points between 30 and 52 MeV for this ratio was 1.03 ± 0.04). We noted above that they used values for β for the (γ, n) reaction which differ appreciably from our adopted values. [The values they used for β for the (γ, p) reaction are virtually identical to those we used.] Had they used the values for the (γ, n) reaction which we used, they would have obtained values for $\sigma(\gamma, p)/\sigma(\gamma, n)$ of 1.15 ± 0.10 (instead of 1.05) at 35.2 MeV, 1.15 ± 0.09 (instead of 1.03) at 37.1 MeV, and 1.09 ± 0.08 (instead of 1.01) at 44.3 MeV.

These and other data points from Ref. 14, re-analyzed with the angular-distribution coefficients of Table I, also are shown in Fig. 7. The point at 44.3 MeV is the one that is most at issue here. Dodge and Murphy give no other result between 37.1 and 51.8 MeV, in the energy region of the apparent minimum in the cross-section ratio shown in Fig. 7, whereas the value which can be assigned to a smooth approximation to our data in a ± 1 -MeV energy interval (say) near 44 MeV is at least two standard deviations below that of Ref. 14. Thus, even though another measurement of the photoneutron angular distribution in this energy region, preferably with monoenergetic photons, clearly is called for, this discrepancy will remain. One also can ask whether effects of $E2$ or other multipolarities are playing an important role here, and have not been taken properly into account in the virtual-photon analysis of Ref. 14. (It is well known^{28,29} that $E2$ and $M1$ transitions are enhanced in electroexcitation when the energy of the incident electron exceeds greatly the excitation energy, and a 90-MeV electron beam was used in Ref. 14. High incident electron energies were used for some of the measurements of Ref. 22 as well.) However, one would not expect a large error from this cause alone for such a low- Z nucleus. It appears, therefore, that however one treats the angular

distributions or the virtual-photon analysis, a discrepancy will remain between the present results and those of Ref. 14 in this energy region.

In sum, we measured the (γ, p) -to- (γ, n) differential cross-section ratio for ${}^4\text{He}$ by detecting the recoil ${}^3\text{H}$ and ${}^3\text{He}$ nuclei at 90° to the direction of the incident photon beam from 31 to 51 MeV. The resulting total cross-section ratio $\sigma(\gamma, p)/\sigma(\gamma, n)$ is near unity at the lower energies, but deviates significantly from unity at the higher energies; in the energy region near 44 MeV, $\sigma(\gamma, n)$ exceeds $\sigma(\gamma, p)$, and near 50 MeV, $\sigma(\gamma, p)$ appears (but with larger experimental uncertainties) to exceed $\sigma(\gamma, n)$. A statistically significant discrepancy is pointed out between our data near 44 MeV and the datum of Dodge and Murphy¹⁴ at that energy. Finally, we note that this experiment was difficult to perform on our low-duty-factor accelerator, and therefore one might hope that another such measurement, using one of the new high-duty-factor accelerators, would improve upon the present results.

This work was performed under the auspices of the U. S. Department of Energy at Lawrence Livermore Laboratory under Contract No. W-7405-ENG-48, and was supported in part by the National Science Foundation. A preliminary account of this work has appeared as Ref. 30.

¹B. L. Berman, S. C. Fultz, and M. A. Kelly, *Phys. Rev. Lett.* **15**, 938 (1970).

²B. L. Berman, S. C. Fultz, and M. A. Kelly, *Phys. Rev. C* **4**, 723 (1971).

³G. A. Ferguson, J. Halpern, R. Nathans, and P. F. Yergin, *Phys. Rev.* **95**, 776 (1954).

⁴A. N. Gorbunov, *Phys. Lett.* **27B**, 436 (1968).

⁵F. Ferrero, C. Manfredotti, L. Pasqualini, G. Piragino, and P. G. Rama, *Nuovo Cimento* **45B**, 273 (1966).

⁶L. Busso, S. Costa, L. Ferrero, R. Garfagnini, L. Pasqualini, G. Piragino, S. Ronchi della Rocca, and A. Zanini, *Lett. Nuovo Cimento* **3**, 423 (1970).

⁷L. Busso, R. Garfagnini, G. Piragino, S. Ronchi della Rocca, and A. Zanini, *Lett. Nuovo Cimento* **1**, 941 (1971).

⁸R. W. Zurmühle, W. E. Stephens, and H. H. Staub, *Phys. Rev.* **132**, 751 (1963).

⁹B. L. Berman, F. W. K. Firk, and C.-P. Wu, *Nucl. Phys.* **A179**, 791 (1972).

¹⁰J. D. Irish, B. L. Berman, R. G. Johnson, B. J. Thomas, K. G. McNeill, and J. W. Jury, in *Proceedings of the International Conference on Few Particle Problems in Nuclear Physics, Los Angeles, California, 1972*, edited by I. Slaus, S. A. Hozzkowski, R. P. Haddock, and W. T. H. van Oers (North-Holland, Amsterdam, 1973), p. 888.

¹¹J. D. Irish, R. G. Johnson, B. L. Berman, B. J. Thomas, K. G. McNeill, and J. W. Jury, *Can. J. Phys.* **53**, 802 (1975).

¹²D. V. Webb, C. K. Malcolm, Y. M. Shin, and D. M. Skopik, in *Proceedings of the International Conference on Photoneuclear Reactions and Applications, Pacific Grove, California*, edited by B. L. Berman (Lawrence Livermore Laboratory, Livermore, California, 1973), p. 149.

¹³C. K. Malcolm, D. V. Webb, Y. M. Shin, and D. M. Skopik, *Phys. Lett.* **47B**, 433 (1973).

¹⁴W. R. Dodge and J. J. Murphy II, *Phys. Rev. Lett.* **28**, 839 (1972).

¹⁵J. D. Irish, R. G. Johnson, B. J. Thomas, B. L. Berman, K. G. McNeill, and J. W. Jury, in *Proceedings of the International Conference on Photoneuclear Reactions and Applications, Pacific Grove, California*, edited by B. L. Berman (Lawrence Livermore Laboratory, Livermore, California, 1973), p. 147.

¹⁶J. D. Irish, R. G. Johnson, B. L. Berman, B. J. Thomas, K. G. McNeill, and J. W. Jury, *Phys. Rev. C* **8**, 1211 (1973).

¹⁷J. D. Irish, R. G. Johnson, K. G. McNeill, and J. W. Jury, *Phys. Rev. C* **9**, 2060 (1974).

¹⁸S. S. Hanna, in *Proceedings of the International Conference on Photoneuclear Reactions and Applications*,

- Pacific Grove, California*, edited by B. L. Berman (Lawrence, Livermore Laboratory, Livermore, California, 1973), p. 417.
- ¹⁸W. E. Meyerhof, M. Suffert, and W. Feldman, Nucl. Phys. A148, 211 (1970).
- ²⁰Yu. M. Arkatov, P. I. Vatsset, V. I. Voloshchuk, V. V. Kirichenko, I. M. Prokhorets, and A. F. Khodyachikh, Yad. Fiz. 12, 227 (1970) [Sov. J. Nucl. Phys. 12, 123 (1971)]; 13, 256 (1971) [13, 142 (1971)].
- ²¹Yu. M. Arkatov, P. I. Vatsset, V. I. Voloshchuk, A. P. Klyucharev, V. L. Marchenko, and A. F. Khodyachikh, Yad. Fiz. 9, 473 (1969) [Sov. J. Nucl. Phys. 9, 271 (1969)].
- ²²J. J. Murphy II, Ph.D. thesis, University of Illinois, 1971 (unpublished).
- ²³G. D. Wait, S. K. Kundu, Y. M. Shin, and W. F. Stubbins, Phys. Letters 33B, 163 (1970).
- ²⁴L. Crone and C. Wertz, Nucl. Phys. A134, 161 (1969).
- ²⁵W. E. Meyerhof and S. Fiarman, in *Proceedings of the International Conference on Photoneuclear Reactions and Applications, Pacific Grove, California*, edited by B. L. Berman (Lawrence Livermore Laboratory, Livermore, California, 1973), p. 385.
- ²⁶F. C. Barker and A. K. Mann, Philos. Mag. 2, 5 (1957).
- ²⁷F. Balestra, E. Bollini, L. Busso, R. Garfagnini, C. Guaraldo, G. Piragino, R. Scrimaglio, and Z. Zanini, Nuovo Cimento 38A, 145 (1977).
- ²⁸W. W. Gargaro and D. S. Onley, Phys. Rev. C 4, 1032 (1971).
- ²⁹I. C. Nascimento, E. Wolyneec, and D. S. Onley, Nucl. Phys. A246, 210 (1975).
- ³⁰T. W. Phillips, D. D. Faul, B. L. Berman, J. R. Calarco, and J. R. Hall, Bull. Am. Phys. Soc. 19, 496 (1979).